

# $G_0W_0$ calculations of optoelectronic properties of Cu- Phthalocyanine crystal for Solar Cell applications

\* Abdullahi Lawal<sup>1</sup>, Ibrahim Buba Garba<sup>2,3</sup>

<sup>1</sup>Department of Physics,  
College of Education Zaria,  
P.M.B 1041, Zaria,  
Kaduna State, Nigeria

<sup>2</sup>Department of Physics,  
Federal University Gashua,  
PMB 1005, Gashua,  
Yobe State, Nigeria.

<sup>3</sup>Institut de Minéralogie,  
de Physique des Matériaux et de Cosmochimie (IMPMC),  
Sorbonne Université  
4 place Jussieu,  
75005 Paris, France.

Email: [abdullahikubau@yahoo.com](mailto:abdullahikubau@yahoo.com)

---

## Abstract

*In this work, structural properties of Cu-Phthalocyanine molecular crystal ( $\beta$ -CuPc) are studied via first-principles approach within density functional theory (DFT) framework. The calculated structural parameters are close to experimental result. Many-body perturbation theory (MBPT) based on convolution of non-interacting Green's function ( $G_0$ ) and a screened Coulomb interaction ( $W_0$ ),  $G_0W_0$  approximation were used for quasiparticle (QP) band structure and optical properties calculations. The bandgap value of 1.71 eV calculated with  $G_0W_0$ +RPA is in good agreement with experimental value. Optical properties calculations show that the results obtained within  $G_0W_0$  plus random phase approximation (RPA) are close to available experimental results. Interestingly, optical gap of 1.71 eV and strong absorption of  $\beta$ -CuPc in the visible light and ultraviolet regions shows that the investigated material is suitable for optoelectronic and solar cells applications.*

**Keywords:** Cu- Phthalocyanine, DFT,  $G_0W_0$ , Optical spectra.

## INTRODUCTION

In order to deal with global energy demand, harvesting solar energy using photovoltaic (PV) technology is considered among the best way (Hernandez et al., 2014, Lawal et al., 2021). Utilization of silicon-based PV for solar cell application remained dominant for decades until energy challenge has been disputed in mankind due to the rise in population and globalization. Hence, a necessity in finding photoactive materials with better performance, lifetime, abundant, cost-effective and environment-friendly are needed to meet the mankind needs. Next, potential active material in replacing silicon is inorganic-based (ISMs) such as

---

\*Author for Correspondence

Gallium Arsenide (GaAs), Cadmium Telluride (CdTe) and Copper-Indium Diselenide (CIS). These ISMs possess better abilities in absorbing solar energy due to their high optical absorption when compared to crystalline silicon (Kippelen and Brédas, 2009). However, the growth of ISM-based for PV is relatively slow due to the challenge in production such as difficulty in controlling the doping and achieving stability, hazardous and thermally unstable (Bharam and Day, 2012). Recently, researchers have diverted their interests to organic semiconductor materials (OSMs). In fact, the optoelectronic device based on OSM is easier and cheaper to fabricate than ISMs (Williams, 2012, Nunzi, 2002, Izawa et al., 2019). Hence, the study of OSMs generally seeks opportunity to dominate in PV technology with enhanced performance over the current market of conventional crystalline silicon and inorganic semiconductor materials. Among the organic materials, Cu-phthalocyanines is chosen in this paper because of its strong absorptions, stability, solubility, good efficiency, and its peculiar conducting properties (Neduvhuledza et al., 2020). Therefore, in order to attain its respective properties, a comprehensive investigation on the structure, electronic and optical properties are needed. In this regard, the use of *ab initio* quantum mechanical computational techniques in performing virtual experiment may lead to a cheaper experiment and shorter developmental cycle. Computational *ab initio* methodologies based on Density Functional Theory (DFT) are intensely used by the theoretical researchers to solve the complex problems. However, fundamental bandgap and optical gap are usually underestimated within such method (Cao et al., 2013). Hence, to overcome this discrepancy between DFT calculations and experimental results, one-particle Green's function based on many-body perturbation theory (MBPT) within non-self-consistent GW approach (one-shot G<sub>0</sub>W<sub>0</sub> approximation) is the most reliable and one of the cheapest methods for computing quasiparticle (QP) band structure/bandgap closer to the experimental value (Shahrokhi and Leonard, 2017, Lawal et al., 2020, Lawal et al., 2018b, Lawal et al., 2021)

In this work, calculations of structural parameters of  $\beta$ -CuPc are performed within the framework of DFT as implemented in Quantum Espresso package (Giannozzi et al., 2009). Electronic and optical properties are calculated using many-body perturbation theory (MBPT) via one-shot G<sub>0</sub>W<sub>0</sub> as implemented in YAMBO package (Marini et al., 2009).

## METHODOLOGY

The calculations presented in this work are performed within two open source simulation packages Quantum Espresso (Giannozzi et al., 2009) and YAMBO (Marini et al., 2009) codes. Quantum Espresso (QE) is a software code under GNU general public license (GPL) for materials modelling and electronic structure calculations based on DFT pseudopotentials. Also, QE interface with YAMBO code for excited state calculation which use DFT results as its input. Yambo simulation package is a plane wave norm-conserving pseudopotential code designed for calculating quasiparticle (QP) energies and optical properties within time-dependent density functional theory (TDDFT) and many-body perturbation theory (MBPT). QP energies are calculated within one-shot G<sub>0</sub>W<sub>0</sub> approximation for self-energy. The optical absorption spectra are computed by solving Bethe-salpeter equation (BSE). Yambo code is chosen in this study because of showing accuracy in band structure and optical properties calculations (Sangalli et al., 2019). Accuracy in band gaps with this approach with experimental measurements is due to many-body perturbation theory (MBPT) by QP concept. Optical properties calculations using Yambo code for number of systems in several studies (Lawal et al., 2018b, Lawal et al., 2019, Idris et al., 2020, Kang and Hybertsen, 2010) show high accuracy approaching experimental values. Electronic structure and optical properties of  $\beta$ -CuPc molecular crystal calculations are performed based on Pseudopotential plane-wave method. Pseudopotential method is chosen in our study because is fast and

efficient as previous shape approximation of the orbitals is not required. Perdew-Burke-Ernzerhof generalized gradient approximation (PBE-GGA) (Perdew et al., 1996) exchange-correlation potential is used for lattice dynamics of  $\beta$ -CuPc. Norm-conserving pseudopotential were used in modeling interactions between ionic core potential and electrons of Cu and N atoms. The Brillouin zone integration is performed using Monkhorst-Pack grid of  $11 \times 10 \times 11$  k-points grids for structural and band structure calculations. 80 Ry cut-offs energy of the plane-wave basis set was used to expand the wave functions and 540 Ry for charge density. Quasiparticle band structure and optical properties of  $\beta$ -CuPc molecular crystal were calculated by G<sub>0</sub>W<sub>0</sub> approximation for the self-energy operator  $\Sigma$ . Specifically, frequency dependence of the dielectric matrix were treated by single one shot G<sub>0</sub>W<sub>0</sub> approximation via Godby-Needs plasmon pole model (Godby and Needs, 1989a, Godby and Needs, 1989b). All many-body perturbation theory (MBPT) calculations were performed via Yambo package (Marini et al., 2009). In the one-shot calculations, Converged results attained by kinetic energy cut-offs of 22 Ry for screening dielectric function with 1800 bands. In the G<sub>0</sub>W<sub>0</sub> approximation, G<sub>0</sub> is built from Kohn-Sham orbitals, and QP energies are obtained as first order perturbation correction. QP energies were obtained by solving Dyson equation perturbatively as:

$$E_n^{QP} = E_{nk} + Z_{nk}(\Sigma(E_{nk}) - V_{nk}^{XC}) \quad (1)$$

where  $E_{nk}$  is PBE-GGA KS energies,  $V_{nk}^{XC}$  is the exchange correlation potential,  $\Sigma$  is the expectation values of the self-energy, and  $Z_{nk}$  is the QP renormalization factor defined as(Shishkin and Kresse, 2007) :

$$1/Z_{nk} = 1 - \left[ \frac{d\Sigma(\omega)}{d\omega} \right]_{\omega=E_{nk}} \quad (2)$$

and the self-energy is split into correlation part and screened-exchange (Shahrokhi and Leonard, 2017):

$$\Sigma = \Sigma_X + \Sigma_C \quad (3)$$

The optical properties of the studied material were computed by the complex dielectric function  $\varepsilon(\omega)$ .

$$\varepsilon(\omega) = \varepsilon_1(\omega) + i\varepsilon_2(\omega) \quad (4)$$

The complex dielectric function is an important function that describes the optical properties of a material. Using Eq. 5 the real part ( $\varepsilon_1(\omega)$ )was calculated by employing the Kramers-Kronig relations while the imaginary part ( $\varepsilon_2(\omega)$ )of the complex dielectric function is obtained by summing transitions from valence (occupied) to conduction (unoccupied) states (with fixed k) over the BZ as shown in Eq. 6(34).

$$\varepsilon_1(\omega) = 1 + \left(\frac{2}{\pi}\right) P \int_0^\infty \frac{\omega' \varepsilon_2(\omega')}{(\omega'^2 - \omega^2)} d\omega' \quad (5)$$

$$\varepsilon_2(\omega) = \frac{16\pi e^2}{\omega^2} \sum_S |\vec{\lambda} \cdot \langle O | \vec{v} | S \rangle|^2 \delta(\omega - E_{ck}^{QP} + E_{vk}^{QP}) \quad (6)$$

where P represents the Cauchy principal value, where  $\vec{\lambda}$  is the polarization vector of light.  $\langle O | \vec{v} | S \rangle$  is the optical transition matrix from valence to conduction states and  $\vec{v}$  is the single-particle velocity operator,  $E_{vk}^{QP}$  and  $E_{ck}^{QP}$  are the QP energies for the valence and conduction band states. The symbols  $\omega$  and  $k$  denote the frequency of incident radiation and momentum operator respectively while the total energy is given by an integral part of Eq. 2. Consequently, with the knowledge of imaginary and real part of microscopic dielectric function other important optical spectra can be calculated (refractive index  $n(\omega)$ , absorption index  $\alpha(\omega)$ , conductivity  $\sigma(\omega)$  electron loss function  $L(\omega)$ , reflectivity  $R(\omega)$  and extinction index  $k(\omega)$ )

## RESULTS AND DISCUSSION

### Structural properties

Figure 1 displayed the optimized  $\beta$ -CuPc molecular crystal structure. The crystalline phase is built in a monoclinic symmetry with the space group of P21/a. During optimization, a powerful system can be a handful since the structure consumed plenty of time and memory in order to fully converge. The obtained lattice parameters of  $\beta$ -CuPc are  $a = 19.849\text{\AA}$ ,  $b = 4.720\text{\AA}$ ,  $c = 14.800\text{\AA}$  with a  $\beta$ -angle of  $122.280^\circ$  and these values are in agreement with previous results (El-Nahass et al., 2002, Brown, 1968).

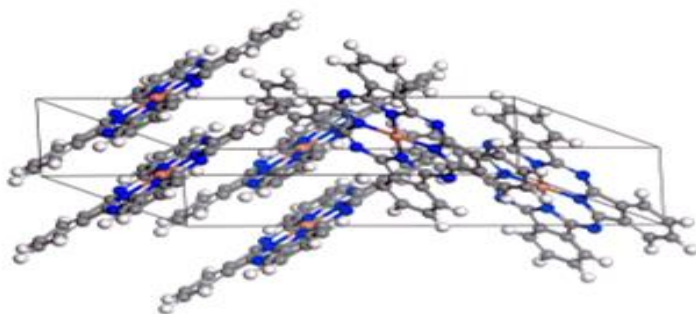


**Figure 1** Schematic view of  $\beta$ -CuPc molecular crystal. The pink, blue, grey, and white colors correspond to copper, nitrogen, carbon and grey atoms respectively.

### Electronic properties

Regardless of the structural properties, the  $\pi$ -interaction that perturbs the electronic and optical properties of  $\beta$ -CuPc is more important to be investigated. The electronic structure calculations of  $\beta$ -CuPc molecular crystal are carried using optimized structure by means of Perdew–Burke–Ernzerhof generalized gradient approximation (PBE-GGA) and  $G_0W_0$  approximation. The band structures were calculated along high-symmetry directions of the irreducible Brillouin zone (BZ) ( $Z \rightarrow \Gamma \rightarrow \Psi \rightarrow A \rightarrow B \rightarrow D \rightarrow E \rightarrow X$ ) and fermi energy level is set at 0 eV. For band structure calculation with PBE, the energy separation between the lowest conduction band and highest valence band was found to be 1.02 eV and this value is consistent with previous DFT result (Sharma et al., 2012). However, the value is smaller than experimental result of 1.7 eV (Hill et al., 2000, Schwieger et al., 2002) and this effect is the limitation of DFT approach due to approximations used in the exchange-correlation potential. It is well known that the standard DFT functional such as GGA always underestimate band gap for the semiconductor compound. As can be seen in Figure 2, the valence band maximum (VBM) lie at the B point and the conduction band minimum (CBM) occurred between B and A points of the first Brillouin-Zone for both (PBE-GGA) and  $G_0W_0$  approaches. This indicates that  $\beta$ -CuPc has indirect energy bandgap. Conversely, the direct and indirect band gaps differ by just 0.07 eV. Therefore, in practical applications, particularly in optoelectronic,  $\beta$ -CuPc can be considered as direct gap semiconductor material. However, to correct this inconsistency of the bare DFT calculation, we further performed  $G_0W_0$  calculation. Interestingly, inclusion of GW potential bring the fundamental band gap value to 1.63 eV and this value is in good agreement with experimental value of 1.7 eV (Hill et al., 2000, Schwieger et al., 2002). The calculated electronic bandgaps along with experimental result are listed in Table 1. To explore further, we calculated the total density of states (TDOS) and partial density of states (PDOS) of  $\beta$ -CuPc. The density of states plays an important role in the formation of bands and the study of the band gap. Results of TDOS will assist to clearly understand the nature of the bands while PDOS provide information about the origin of the bands. The calculated TDOS and PDOS are displayed in Figure 2 (b). The occurrence of the valence band between -10 eV to -5 eV is due to the domination of the

s- and p-s orbitals. The intermediate occurrence of the valence band closer to the Fermi level between -5 eV to 0 eV is due to the domination of the d- and -p orbitals. The lowest unoccupied conduction bands are due to the domination of the d-and p-orbitals. The s-orbital also contribute to the conduction band, but the contributions is very small.

**Table 1.**The energy gaps of  $\beta$ -phase molecular crystal of Cu-phthalocyanine

Methods	Energy gap of $\beta$ -CuPc crystal, E <sub>g</sub> (eV)
GGA-PBE	1.02
G <sub>0</sub> W <sub>0</sub>	1.71
Explement(Hill et al., 2000, Schwieger et al., 2002)	1.70

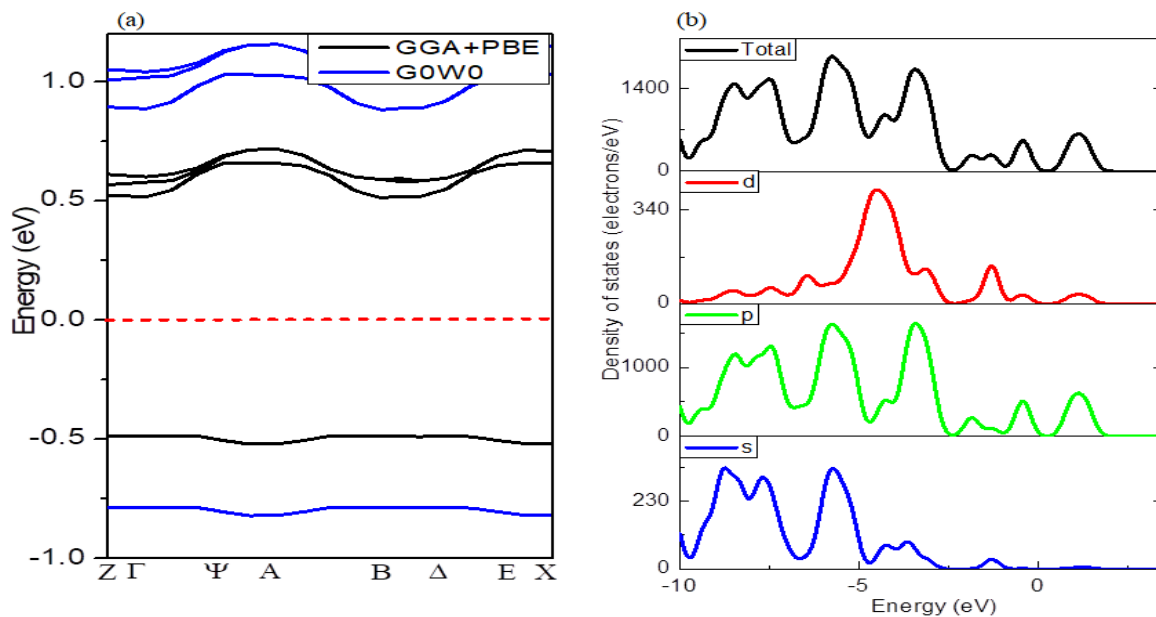


Figure 2(a) Band structure (b) Density of states of  $\beta$ -CuPc molecular crystal

**Optical Properties**

The study of the optical properties of a material is crucial to get insight view about its characteristics for the applications in the optoelectronic system and devices. Optical properties of a material explain the behavior of the material when exposed to electromagnetic radiations. From the comprehensive literature review, it is found that the exploration of the optical features relating to Cu-Phthalocyanine is scarcely done.(Rahdar et al., 2012). The optical properties of  $\beta$ -CuPc molecular crystal is computed using random phase approximation (RPA) based on G<sub>0</sub>W<sub>0</sub> (G<sub>0</sub>W<sub>0</sub>+RPA). Although optical properties calculation using G<sub>0</sub>W<sub>0</sub>+RPA is computationally expensive, but it provides accurate description of absorption spectra. The optical parameters considered in this paper are imaginary  $\epsilon_2(\omega)$  and real  $\epsilon_1(\omega)$  parts of dielectric functions, optical conductivity,  $\sigma(\omega)$  and absorption coefficient,  $\alpha(\omega)$ . The real part  $\epsilon_1(\omega)$  of frequency dependent of the dielectricfunction provides the energy stored in material whereas imaginary part  $\epsilon_2(\omega)$  of frequency dependent of the dielectric function is concerned with the absorption behavior and the electronic band structure of the material under investigation. Figure 3 (a) shows a result of real part of frequency dependent of the dielectric function of  $\beta$ -CuPc. The real part of frequency dependent of the dielectric function of  $\beta$ -CuPc presents significant results, where at 0eV it possesses a dielectric coefficient value of 3.44which is called static dielectric

constant  $\epsilon_1(0)$ . Our calculated static dielectric constant of 3.44 is in good agreement with experimental value of 3.51 (Forrest et al., 1989). Static dielectric constant  $\epsilon_1(0)$  in low energy limit strongly depends on the band gap value of the material. With the help of screened plasma frequency (plasma energy), this value can be used to find the band gap value of the compound via Penn Model (Penn, 1962) as shown in Eq 7.

$$\epsilon(0) = \left(\frac{\hbar\omega_p}{E_g}\right)^2 + 1 \quad (7)$$

Figure 3 (b) shows a graph of imaginary part of frequency dependent dielectric function. The first critical point sometimes called edge of optical absorption occurred at about 1.71 eV and this value is in good agreement with experimental results (Hill et al., 2000, Schwieger et al., 2002) of 1.5 eV (Haidu et al., 2013, Schwieger et al., 2002). This point splits the valence band maximum and conduction band minimum and is known as the fundamental absorption edge (Lawal et al., 2018a, Lawal et al., 2017, Lawal et al., 2018b). The transitions from different occupied states in the valence bands to different unoccupied states in conduction bands or higher empty orbitals generate several weak peaks. The highest peak appears at 2.91 eV indicating that  $\beta$ -CuPc is a promising candidate for optoelectronic applications. The value of optical gap, reflectivity and static dielectric function together with experimental data are presented in Table 2. Remarkably,  $\beta$ -CuPc has strong absorption in the visible light region that depicts the appropriateness for solar cells application.

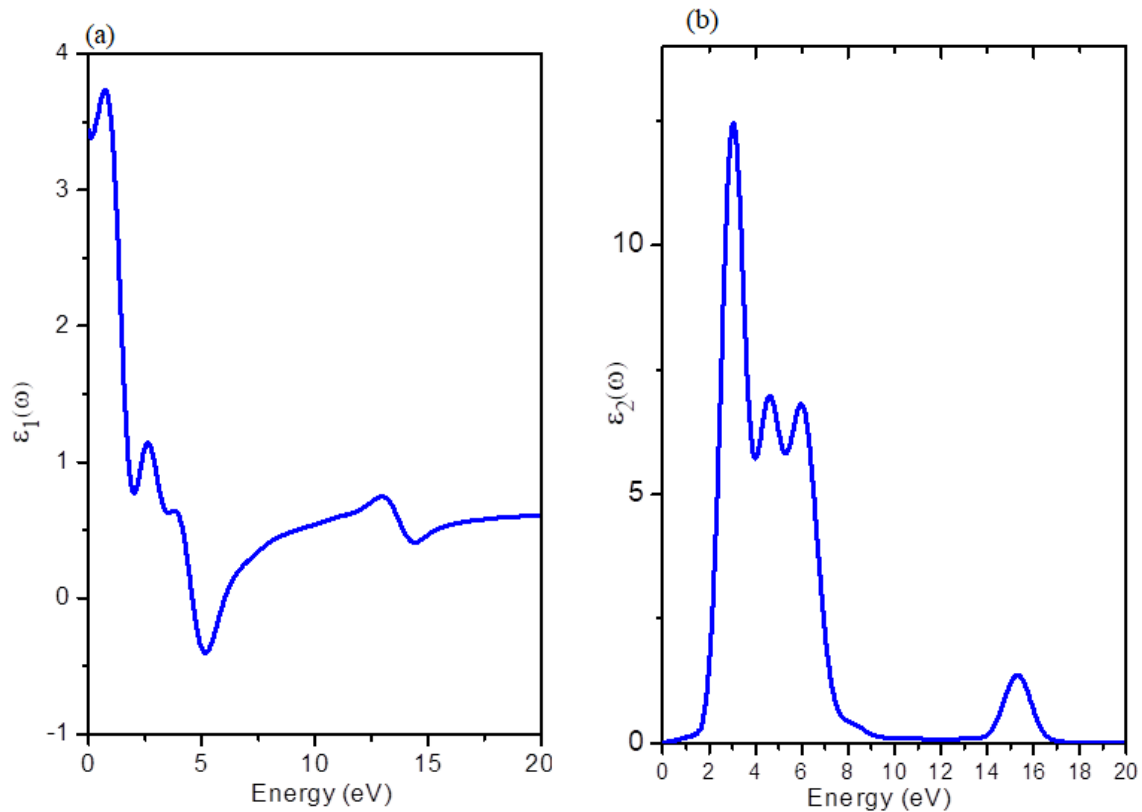


Figure 3 (a) Real part part of the dielectric function (b) Imaginary part of the dielectric function of  $\beta$ -CuPc

Table 2:  $\beta$ -CuPc G<sub>0</sub>W<sub>0</sub>+RPA results compared with experimental measurements

		Optical gap (eV)	Reflectivity	$\epsilon(\infty)$
Our work	G <sub>0</sub> W <sub>0</sub> +RPA	1.71	2.91	3.44
	Experiments	1.70(Hill et al., 2000, Schwieger et al., 2002)	2.87 (Singh and Ravindra, 2010)	3.5 (Forrest et al., 1989)

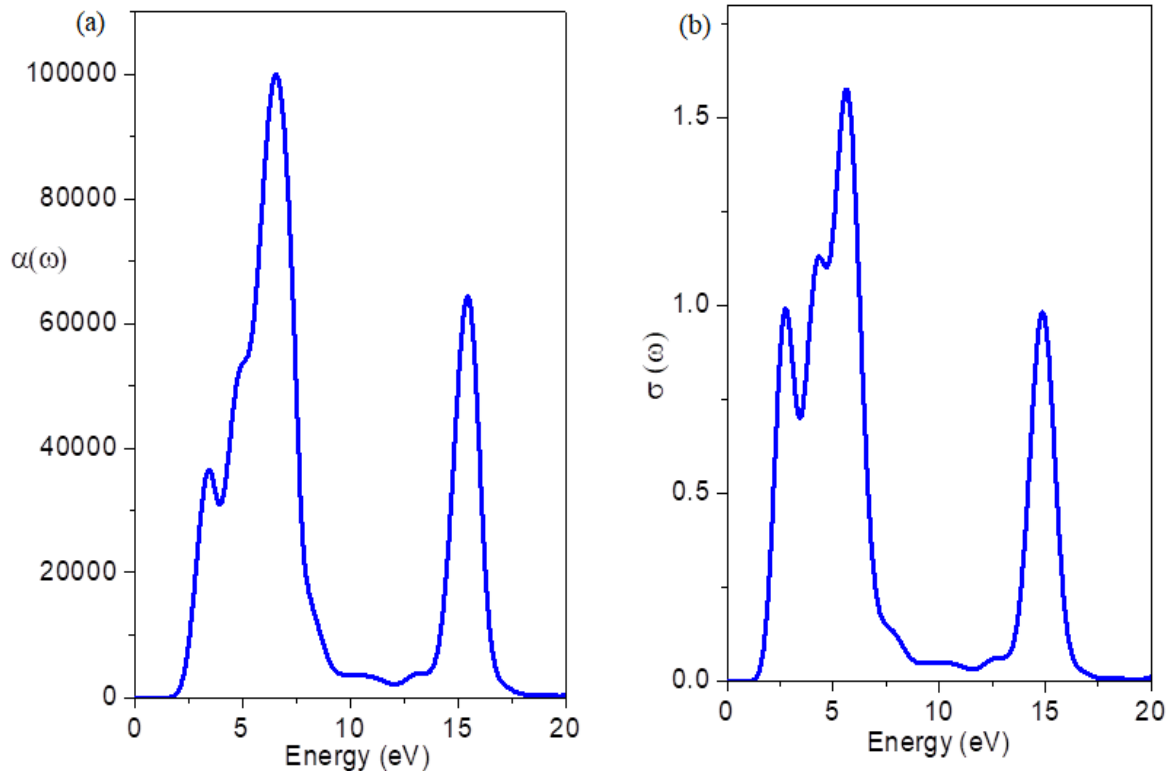


Figure 4 (a) Absorption coefficient (b) Optical Conductivity calculated

Figure 4 (a) shows the frequency dependent absorption coefficient  $\alpha(\omega)$ . When light rays strike the surface of a material, part of it as energy is transferred to the surface while some are reflected back. This transfer of energy to the surface is called absorption of light. From Figure 4 (a), we can say that  $\beta$ -CuPc has good absorption coefficient value for visible light region and highest value of absorption coefficient appears at 5.3 eV. Since  $\beta$ -CuPc exhibit good absorption coefficient in UV/visible range, therefore, it can be used in optoelectronics devices and as solar cell material (Hosokawa et al., 2001). Within the energy range between 0.0 eV to 1.62 eV, the  $\alpha(\omega)$  is zero, and this indicates an absence of interaction between the medium and the incident photon. Our theoretical study on  $\beta$ -CuPc molecular crystal for the first time with accurate method shows that it has an optical gap of 1.62 eV and thus can be used for optoelectronic applications particularly solar cells. This suggests that a device fabricated from this material can be operated on a wide range of the energy scale. Figure 4 (b) shows the optical conductivity  $\sigma(\omega)$  for  $\beta$ -CuPc. Optical conductivity is a measurement of photoconductivity that gives information about electrical conductivity in any material under investigation and it is related to absorption spectrum. The frequency variation is described by energy between 0 to 20 eV. The material's conductivity increases as the energy increases and from 2 eV to 7.5 eV the material under investigation it has the highest values of conductivity. Figure 5(a) represents the reflectivity of  $\beta$ -CuPc and it can be seen that  $\beta$ -CuPc has high reflectivity in the visible light range. The first edge of reflectivity was found to be 2.91 and this value agreed well with experimental value of 2.89 (Singh and Ravindra, 2010). This result indicates that the  $\beta$ -CuPc is transparent for photon energy less than 5 eV

which is appropriate for applications in visible light region. Energy loss function  $L(\omega)$  is an important factor that measures the energy dissipation of a fast-moving electron within the medium. The energy loss function  $L(\omega)$  gives the energy loss of fast moving electrons in solids (Snoke, 2020, Kittel et al., 1996, Kittel, 1966). The graph of energy loss function is represented in Figure 5(b). This graph gives information about loss in energy of absorbed spectrum. Energy loss is indicated for UV region and maximum energy is lost at 9.3 eV . Energy loss could be due to inelastic interactions, intra and inter intra band transitions, inner shell ionization, and phonon excitations. The effect of loss function on absorption represents in Figure 4 (a). In this graph, we can see that absorption coefficients show minimum value where energy loss function shows highest value. Now we can conclude that  $\beta$ -CuPc molecular crystal has good absorbance for UV range in addition to visible light.

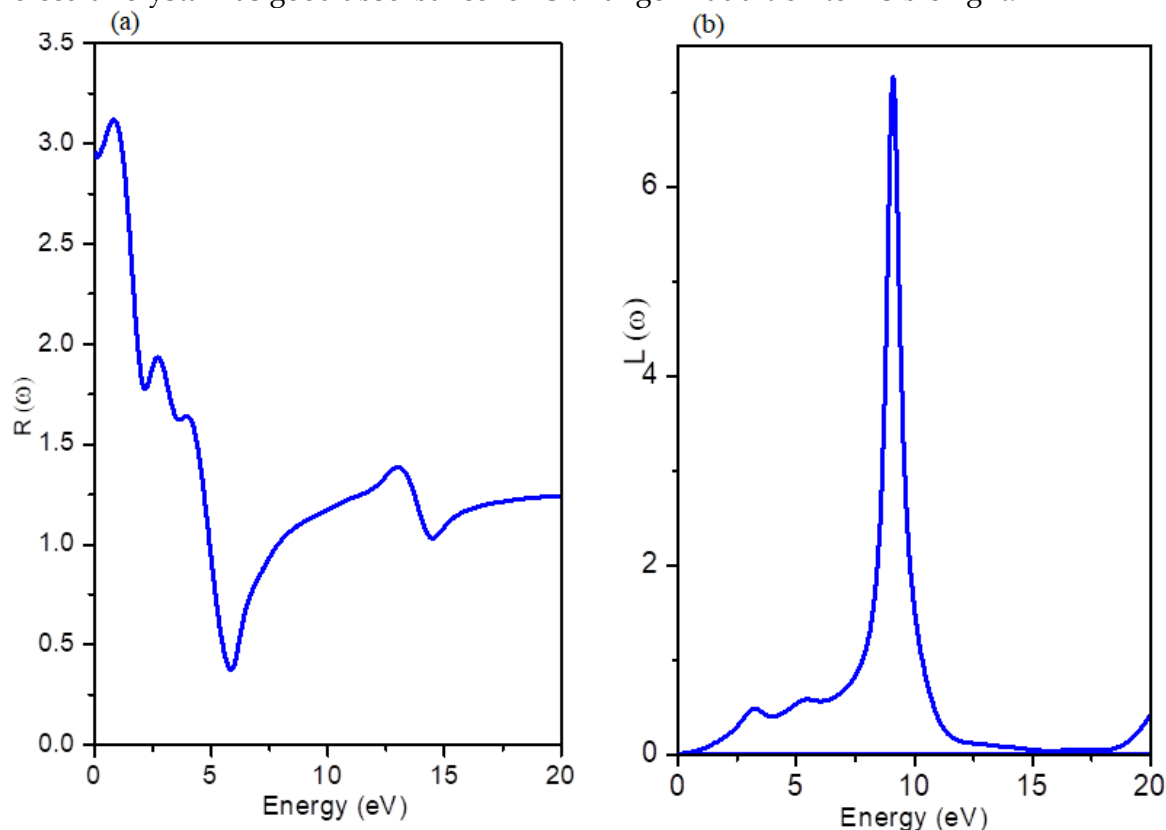


Figure 5 (a) Reflectivity (b) Electron loss function

## CONCLUSION

In summary, we have presented optoelectronic properties of  $\beta$ -CuPc molecular crystal. First-principles calculations of the DFT as implemented in quantum Espresso was adopted. The calculated structural parameters are close to experimental results. The investigated electronic band structure reveals that  $\beta$ -CuPc molecular crystal is an indirect bandgap material. We found the band gap value in this work to be 1.02 eV and 1.71 eV using GGA+PBE and G<sub>0</sub>W<sub>0</sub>. The electronic bandgap value calculated with G<sub>0</sub>W<sub>0</sub>+RPA is in good agreement with experimental data. In addition to electronic properties, optical parameters is performed by evaluating dielectric function  $\epsilon(\omega)$  via RPA based on G<sub>0</sub>W<sub>0</sub>. Optical properties calculations show that the results obtained within G<sub>0</sub>W<sub>0</sub>+RPA are in good agreement with available experiments. Interestingly, optical gap of 1.71 eV and strong absorption of  $\beta$ -CuPc in the visible light and ultraviolet regions shows that the investigated material is suitable for optoelectronic and solar cells applications.

**REFERENCES**

- Dharam, V. & Day, D. 2012. Advantages and challenges of silicon in the photovoltaic cells.
- Brown, C. 1968. Crystal structure of  $\beta$ -copper phthalocyanine. *Journal of the Chemical Society A: Inorganic, Physical, Theoretical*, 2488-2493.
- Cao, Y., Waugh, J., Zhang, X., Luo, J.-W., Wang, Q., Reber, T., Mo, S., Xu, Z., Yang, A. & Schneeloch, J. 2013. Mapping the orbital wavefunction of the surface states in three-dimensional topological insulators. *Nature Physics*, 9, 499-504.
- El-Nahass, M., Bahabri, F., Ghamdi, A. & Al-Harbi, S. 2002. Structural and transport properties of copper phthalocyanine (CuPc) thin films. *Egypt. J. Sol*, 25, 307-321.
- Forrest, S., Leu, L., So, F. & Yoon, W. 1989. Optical and electrical properties of isotype crystalline molecular organic heterojunctions. *Journal of applied physics*, 66, 5908-5914.
- Giannozzi, P., Baroni, S., Bonini, N., Calandra, M., Car, R., Cavazzoni, C., Ceresoli, D., Chiarotti, G. L., Cococcioni, M. & Dabo, I. 2009. QUANTUM ESPRESSO: a modular and open-source software project for quantum simulations of materials. *Journal of physics: Condensed matter*, 21, 395502.
- Godby, R. & Needs, R. 1989a. Metal-insulator transition in Kohn-Sham theory and quasiparticle theory. *Physical review letters*, 62, 1169.
- Godby, R. & Needs, R. 1989b. The metal-insulator transition in quasiparticle theory and Kohn-Sham theory. *Physical Review Letters*, 62, 1169-1172.
- Haidu, F., Fechner, A., Salvan, G., Gordan, O., Fronk, M., Lehmann, D., Mahns, B., Knupfer, M. & Zahn, D. 2013. Influence of film thickness and air exposure on the transport gap of manganese phthalocyanine. *AIP Advances*, 3, 062124.
- Hernandez, R., Easter, S., Murphy-Mariscal, M., Maestre, F., Tavassoli, M., Allen, E., Barrows, C., Belnap, J., Ochoa-Hueso, R. & Ravi, S. 2014. Environmental impacts of utility-scale solar energy. *Renewable and Sustainable Energy Reviews*, 29, 766-779.
- Hill, I., Kahn, A., Soos, Z. & Pascal Jr, R. 2000. Charge-separation energy in films of  $\pi$ -conjugated organic molecules. *Chemical Physics Letters*, 327, 181-188.
- Hosokawa, Y., Yashiro, M., Asahi, T. & Masuhara, H. 2001. Photothermal conversion dynamics in femtosecond and picosecond discrete laser etching of Cu-phthalocyanine amorphous film analysed by ultrafast UV-VIS absorption spectroscopy. *Journal of Photochemistry and Photobiology A: Chemistry*, 142, 197-207.
- Idris, M., Shaari, A., Razali, R., Lawal, A. & Ahams, S. 2020. Investigation of self-consistent site-dependent DFT+ U effect on electronic band structure and optical properties of SiFe<sub>2</sub>O<sub>4</sub> spinel. *Materials Research Express*, 7, 026304.
- Izawa, S., Perrot, A., Lee, J.-H. & Hiramoto, M. 2019. Organic pn homojunction solar cell. *Organic Electronics*, 71, 45-49.
- Kang, W. & Hybertsen, M. S. 2010. Quasiparticle and optical properties of rutile and anatase TiO<sub>2</sub>. *Physical Review B*, 82, 085203.
- Kippelen, B. & Brédas, J.-L. 2009. Organic photovoltaics. *Energy & Environmental Science*, 2, 251-261.
- Kittel, C. 1966. *Introduction to Solid State Physics. [With Illustrations.]*, John Wiley & Sons.
- Kittel, C., Mceuen, P. & Mceuen, P. 1996. *Introduction to solid state physics*, Wiley New York.
- Lawal, A., Shaari, A., Ahmed, R. & Jarkoni, N. 2017. First-principles investigations of electron-hole inclusion effects on optoelectronic properties of Bi<sub>2</sub>Te<sub>3</sub>, a topological insulator for broadband photodetector. *Physica B: Condensed Matter*, 520, 69-75.
- Lawal, A., Shaari, A., Ahmed, R. & Jarkoni, N. 2018a. Electronic and Optical Properties of Bi<sub>2</sub>Se<sub>3</sub> Topological Insulator by First Principles Approach for Broadband Photodetector. *Advanced Science Letters*, 24, 3597-3601.
- Lawal, A., Shaari, A., Ahmed, R. & Taura, L. 2018b. Investigation of excitonic states effects on optoelectronic properties of Sb<sub>2</sub>Se<sub>3</sub> crystal for broadband photo-detector by highly accurate first-principles approach. *Current Applied Physics*, 18, 567-575.

- Lawal, A., Shaari, A., Ahmed, R., Taura, L., Madugu, L. & Idris, M. 2019. Sb<sub>2</sub>Te<sub>3</sub>/graphene heterostructure for broadband photodetector: A first-principles calculation at the level of Cooper's exchange functionals. *Optik*, 177, 83-92.
- Lawal, A., Shaari, A., Taura, L., Radzwan, A., Idris, M. & Madugu, M. 2021. G<sub>0</sub>W<sub>0</sub> plus BSE calculations of quasiparticle band structure and optical properties of nitrogen-doped antimony trisulfide for near infrared optoelectronic and solar cells application. *Materials Science in Semiconductor Processing*, 124, 105592.
- Lawal, A., Taura, L. S. & Madugu, M. 2020. Quasiparticle Effects in Bulk and Monolayer of CuSbS<sub>2</sub> Band Structure for Solar Cells and Optoelectronic Application. *SLU Journal of Science and Technology*, 1, 73-79.
- Marini, A., Hogan, C., Grüning, M. & Varsano, D. 2009. Yambo: an ab initio tool for excited state calculations. *Computer Physics Communications*, 180, 1392-1403.
- Neduvhuledza, Z., Nkaki, T., Louzada, M., Nyokong, T. & Khene, S. 2020. Photophysical and nonlinear optical properties of the positional isomers of 4-(4-tertbutylphenoxy) substituted cobalt, nickel and copper phthalocyanines. *Optical Materials*, 109, 110195.
- Nunzi, J.-M. 2002. Organic photovoltaic materials and devices. *C. R. Physique* 3, 523-542.
- Penn, D. R. 1962. Wave-number-dependent dielectric function of semiconductors. *Physical Review*, 128, 2093.
- Perdew, J. P., Burke, K. & Wang, Y. 1996. Generalized gradient approximation for the exchange-correlation hole of a many-electron system. *Physical Review B*, 54, 16533.
- Rahdar, A., Eivari, H. A. & Sarhaddi, R. 2012. Study of structural and optical properties of ZnS: Cr nanoparticles synthesized by co-precipitation method. *Indian Journal of Science and Technology*, 5, 1855-1858.
- Sangalli, D., Ferretti, A., Miranda, H., Attaccalite, C., Marri, I., Cannuccia, E., Melo, P., Marsili, M., Paleari, F. & Marrazzo, A. 2019. Many-body perturbation theory calculations using the yambo code. *arXiv preprint arXiv:1902.03837*.
- Schwieger, T., Peisert, H., Golden, M., Knupfer, M. & Fink, J. 2002. Electronic structure of the organic semiconductor copper phthalocyanine and K-CuPc studied using photoemission spectroscopy. *Physical Review B*, 66, 155207.
- Shahrokhi, M. & Leonard, C. 2017. Tuning the band gap and optical spectra of silicon-doped graphene: Many-body effects and excitonic states. *Journal of Alloys and Compounds*, 693, 1185-1196.
- Sharma, Y., Srivastava, P., Dashora, A., Vadkhiya, L., Bhayani, M., Jain, R., Jani, A. & Ahuja, B. 2012. Electronic structure, optical properties and Compton profiles of Bi<sub>2</sub>S<sub>3</sub> and Bi<sub>2</sub>Se<sub>3</sub>. *Solid State Sciences*, 14, 241-249.
- Shishkin, M. & Kresse, G. 2007. Self-consistent G W calculations for semiconductors and insulators. *Physical Review B*, 75, 235102.
- Singh, P. & Ravindra, N. 2010. Optical properties of metal phthalocyanines. *Journal of materials science*, 45, 4013-4020.
- Snoke, D. 2020. *Solid state physics: Essential concepts*, Cambridge University Press.
- Williams, A. 2012. *Organic PV: can UK start-ups carve out a niche?* [Online]. SPIE. Available: <http://optics.org/indepth/3/6/2> [Accessed].